A benzothiazole-based fluorescence turn-on sensor for copper(II)

Gyeongjin Kim
Seoul National University of Science and Technology
Donghwan Choi
Seoul National University of Science and Technology
Cheal Kim (chealkim@snut.ac.kr)
Seoul National University of Science and Technology https://orcid.org/0000-0002-8692-2457

Research Article

Keywords: benzothiazole, fluorescence chemosensor, copper ion, turn on

Posted Date: April 12th, 2021

DOI: https://doi.org/10.21203/rs.3.rs-381861/v1

Abstract

A new benzothiazole-based chemosensor **BTN** (1-((Z)-(((E)-3-methylbenzo[d]thiazol-2(3H)-ylidene)hydrazono)methyl)naphthalen-2-ol) was synthesized for the detection of Cu^{2+}. **BTN** could detect Cu^{2+} with “off-on” fluorescent response from colorless to yellow irrespective of presence of other cations. Limit of detection for Cu^{2+} was determined to be 3.3 μM. Binding ratio of **BTN** and Cu^{2+} turned out to be a 1:1 with the analysis of Job plot and ESI-MS. Sensing feature of Cu^{2+} by **BTN** was explained with theoretical calculations, which might be owing to internal charge transfer and chelation-enhanced fluorescence processes.

1. Introduction

Copper is one of the pivotal transition metals in human body [1–3]. It exists diverse enzymes like cytochrome oxidase and tyrosine, and plays an essential key role in vital metabolisms, such as redox system and physiological response [4]. However, excessive level of copper can cause neurodegenerative troubles like Parkinson's, Wilson's and Alzheimer's disease [5–7]. Furthermore, copper can also be a major source of environmental pollutants because it is widely used in industrial and agricultural practices [8]. Accordingly, it is essential to develop probes that can selectively detect copper with high sensitivity, selectivity and quick response.

Till now, a number of fluorescence chemosensors detecting Cu^{2+} have been developed because of the features such as great selectivity, versatility, sensitivity and relatively simple handling [9–13]. However, many fluorescent sensors for detecting Cu^{2+} are based on “turn-off” system, owing to the paramagnetic character of Cu^{2+} [14]. Therefore, less examples were reported for fluorescence “turn-on” for detecting Cu^{2+} [15]. Fluorescence sensors which have “turn-on” system shows better sensing properties at their sensitivity, selectivity and easy observation than “turn-off” system [16–18]. Moreover, the fluorescence “turn-off” system induced by a fluorescence quenching may give false results from other quenchers in practical samples and then, is less suitable for analytical applications [19]. Thus, the development of “turn-on” chemosensors for Cu^{2+} has been receiving substantial attention.

Many chromophore/fluorophore systems such as quinoline [20, 21], rhodamine [22], bis-thiophene [23], phenazine [24], thiazole ring [25] and BODIPY [26] have been reported and developed for sensing Cu^{2+}. Among the systems, benzothiazole and its derivatives are sometimes used for the design of fluorescent probes due to the features of large Stokes shift and good quantum yield [27, 28]. Meanwhile, naphthol group is a good fluorophore that can interact with various metal ions [29–31]. Thus, the sensor containing both benzothiazole and naphthol moieties might be a suitable platform that can detect Cu^{2+} with turn-on system [32–41].

Herein, we demonstrated the design and application of a “turn-on” fluorescence probe (**BTN)** for detecting Cu^{2+}. In particular, **BTN** can sense selectively Cu^{2+} in samples with metal ions like Hg^{2+}, Fe^{3+}, Co^{2+} and

Ni^{2+} having a fluorescent quenching property. The sensing mechanism and binding structure of **BTN** toward Cu^{2+} were explained by using Job plot, FT-IR, ESI-MS analysis and theoretical calculations

2. Experiments

2.1 General information

^{1}H and ^{13}C NMR were recorded using a Varian spectrometer. Using the Perkin Elmer spectrometers, absorption and fluorescent spectral data were obtained. ESI-mass was provided by an ACQUITY QDa. FT-IR spectra were recorded on Agilent Cary 670 spectrometer.

2.2 Synthesis of BTN (1-((Z)-(((E)-3-methylbenzo[d]thiazol-2(3H)-ylidene)hydrazono) methyl)naphthalen-2-ol)

(E)-2-hydrazono-3-methyl-2,3-dihydrobenzo[d]thiazole (0.11 g, $5x10^{-4}$ mol) was dissolved in methanol (5 mL) and 2-hydroxy-1-naphthaldehyde (0.09 g, $5.1x10^{-4}$ mol) was added into the solution. The light yellow power was immediately formed and the reaction mixture was stirred for 3 h at 22 ^{o}C. The product was filtered and washed with dichloromethane and ether (yield: 78%). ^{1}H NMR (DMSO-d_6), δ (ppm): 12.31 (s, 1H), 9.43 (s, 1H), 8.50 (d, J = 8.8 Hz, 1H), 7.90 (m, 2H), 7.74 (d, *J* = 7.6 Hz, 1H), 7.55 (m, 1H), 7.39 (m, 3H), 7.25 (d, J = 8.8 Hz, 1H), 7.16 (s, 1H), 3.65 (s, 3H). ^{13}C NMR (DMSO-d_6), δ (ppm):164.6 (1C), 158.0 (1C), 151.9 (1C), 140.8 (1C), 132.5 (1C), 131.6 (1C), 128.8 (1C), 127.8 (1C), 127.6 (1C), 126.9 (1C), 123.5 (1C), 122.6 (1C), 122.3 (1C), 122.1 (1C), 121.5 (1C), 117.6 (1C), 110.5 (1C), 109.2 (1C), 31.0 (1C). ESI-mass for [**BTN** + H^{+} + 2·MeCN]$^{+}$, calcd, 416.15 (m/z); found, 415.77.

2.3 Fluorescent and UV-visible tests

Fluorescent and UV-visible tests were checked in acetonitrile. A **BTN** stock (5 mM) was made in DMSO (1 mL) and 6 μL of **BTN** (5 mM) was diluted with 2.997 mL of MeCN to make 10 μM. In titration experiments, 0.75–10.5 μL of a stock $Cu(NO_3)_2$ ($2x10^{-2}$ M) in MeCN were added to **BTN** ($2x10^{-5}$ M). After mixing the solutions for 3 sec, UV-vis and fluorescence spectra were obtained.

2.4 Quantum yield

To compare the quantum yields of **BTN** and **BTN**-Cu^{2+}, fluoresceine (Φ = 0.54 in 100 mM H_2SO_4 solution) was used as reference fluorophore [42]. With the following equation, quantum yield was calculated [42].

$$\Phi_{FS} = \Phi_{FR} \times \frac{A_R \times F_S}{A_S \times F_R} \times \left(\frac{n_S}{n_R}\right)^2$$

(Φ_F = fluorescence quantum yield, F = integrated fluorescence emission, A = absorbance, n = refractive index of the solution, R = reference material and S = test sample)

2.5 Job plot

BTN (1.7 mg, 5 x 10^{-3} mmol) was diluted in DMSO (1 mL). Copper(II) nitrate (47.4 mg, 4 x 10^{-4} mol) was dissolved in 10.0 mL of CH_3CN. To make 20 mL of Cu^{2+} solution (20 μM) and 20 mL of **BTN** solution (20 μM), 80 μL of the stock **BTN** (5x10^{-3} M) was diluted in 19.92 mL of CH_3CN. Likewise, 20 μL of the stock Cu^{2+} (20 mM) was diluted in 19.98 mL of CH_3CN. Then, 0.3-2.7 mL of **BTN** were added to each quartz. 0.3-2.7 mL of Cu^{2+} was added into the quartz to give a total 3 mL volume. After stirring them for 3 sec, fluorescence measurements were executed.

2.6 Competition test

A **BTN** stock (5 mM) was made in DMSO (1 mL). In cells with 3 mL of MeCN, 12 μL of other metal ion stocks (In^{3+}, Fe^{2+}, K^{+}, Fe^{3+}, Al^{3+}, Mn^{2+}, Ga^{3+}, Zn^{2+}, Ni^{2+}, Cd^{2+}, Mg^{2+}, Na^{+}, Cr^{3+}, Hg^{+}, Ag^{2+}, Co^{2+}, Ca^{2+} and Pb^{2+}; 20 mM) was diluted into each cell to make 8 equiv. 12 μL of Cu^{2+} (2x10^{-2} M) was added into each cell. Then, 6 μL of **BTN** (5x10^{-3} M) was added into the cell, which was stirred for a few seconds.

2.7 Theoretical studies

Calculations were executed with Gaussian 16 program [43]. DFT method was applied for geometry optimizations [44, 45]. B3LYP was used for the hybrid functional, and the 6-31G (d,p) basis set was applied to all atoms except for Cu^{2+} [46, 47]. For **BTN**-Cu^{2+} complex, the LANL2DZ basis set was employed for applying effective core potential to Cu^{2+} [48–50]. Imaginary frequencies were not found for both **BTN** and **BTN**-Cu^{2+}, representing the local minima of the structures. The solvent effect of acetonitrile was regarded with IEFPCM [51]. With energy-optimized forms of **BTN** and **BTN**-Cu^{2+}, the possible UV-vis transition states were calculated by using TD-DFT method with twenty lowest singlet states.

3. Results And Discussion

Compound **BTN** was produced by the coupling reaction between 2-hydroxy-1 naphthaldehyde and (E)-2-hydrazono-3-methyl-2,3-dihydrobenzo[d]thiazole (Scheme 1). **BTN** was confirmed by ^{1}H and ^{13}C NMR and ESI-MS (Figs. S1-S3).

3.1 Fluorescent sensing of BTN to Cu^{2+}

The fluorescence spectral measurements to varied metal ions were executed to confirm the fluorescence sensing capability of **BTN** (Fig. 1). **BTN** showed little fluorescence emission. After the addition of Cu^{2+} to **BTN**, the fluorescence emission at 539.5 nm remarkably increased (λ_{ex} = 397 nm) and its solution color

varied to yellow under UV light. Quantum yields of **BTN** and **BTN**-Cu^{2+} were given to be 0.0778 and 0.7919, respectively. By contrast, the presence of other cations with **BTN** did not show any variation.

To find out the sensing process of **BTN** towards Cu^{2+}, fluorescent titration was carried out (Fig. 2). With addition of Cu^{2+}, the fluorescence at 539.5 nm was consistently enhanced. UV-vis spectral tests were carried out to demonstrate the binding property of **BTN** and Cu^{2+} (Fig. 3). The absorbance at 300 and 500 nm significantly increased and that at 380 nm gradually decreased. An obvious isosbestic point observed at 420 nm meant that the binding of **BTN** with Cu^{2+} produced a single product.

The Job plot was executed to investigate the complexation ratio of **BTN** and Cu^{2+} (Fig. 4). It displayed a 1:1 complexation ratio of **BTN** and Cu^{2+}, which was verified by ESI-MS (Fig. S4). The peak of 435.87 (m/z) was expressive to [**BTN** -H^+ + MeCN + Cu^{2+}]$^+$ (calcd; 436.04). Additionally, to illustrate the binding structure of **BTN** with Cu^{2+}, the FT-IR investigation was performed (Fig. S5). The broad O-H peak (2800–3200 cm^{-1}) disappeared after the complexation of **BTN**-Cu^{2+}, demonstrating that the hydroxy group in **BTN** was deprotonated. The C = N peak at 1614 cm^{-1} shifted to 1574 cm^{-1} after **BTN** was bound to Cu^{2+}. These outcomes illustrated that the sulfur, the nitrogen and the deprotonated oxygen of **BTN** might coordinate to Cu^{2+} (Scheme 2). An association constant of **BTN** with Cu^{2+} was analyzed to be 2.0×10^3 M^{-1} (R^2 = 0.9906) with the equation of Benesi-Hildebrand [52] (Fig. S6). With the fluorescence titration, detection of limit for Cu^{2+} turned out to be 3.3 μM using 3σ/K (Fig. 5) [53]. This is only the fourth benzothiazole-based fluorescent “turn-on” probe for detecting Cu^{2+}, while the number of benzothiazole-based fluorescent “turn-off” sensors have been reported (Table S1).

Competitive test was executed to confirm a sensing capability of **BTN** (Fig. 6). **BTN** was not interfered by other cations and exhibited the constant fluorescence emission at 539.5 nm. This indicated that **BTN** can detect Cu^{2+} without being disturbed by other metal ions, resulting in high selectivity. Therefore, **BTN** could be a very effective fluorescence sensor for sensing Cu^{2+} in samples containing other metal ions.

3.2 Calculations

Optimized forms of **BTN** and **BTN**-Cu^{2+} were calculated, based on the Job plot, ESI-mass and IR data (Fig. 7). **BTN** has a distorted structure with bending of the naphthol group, while **BTN**-Cu^{2+} exhibits a nearly planar structure. With the structural change during the complex formation, the dihedral angle (1S, 2N, 3N, 4O) changed from 154.190° to 18.894°.

With energy-optimized forms of **BTN**-Cu^{2+} and **BTN**, TD-DFT calculations were executed to investigate molecular orbitals and transition energies. For **BTN**, the major absorption band stemmed from the HOMO → LUMO transition (380.48 nm, Figs. S7 and S8), which meant intramolecular charge transfer (ICT) from the benzothiazole group to the naphthol one. With **BTN**-Cu^{2+}, the main transition at 427.12 nm stemmed from the HOMO → LUMO (α) and HOMO → LUMO + 1 (β), which showed ICT characteristics (Fig. S9 and S10). Given the experiment and calculation results, the fluorescent turn-on process of **BTN** to Cu^{2+} may

be CHEF effect [54, 55]. Free vibration and rotation of **BTN**, non-radiative transitions, were restricted due to the complex formation with Cu^{2+}. The red shift shown in the experimental UV-vis spectra was consistent with the decreased energy gap. Based on calculations and experimental results, proper structure of **BTN**-Cu^{2+} was proposed (Scheme 2).

4. Conclusion

We presented a great efficient fluorescent turn-on chemosensor **BTN** synthesized from the combination of 3-methyl-2-benzothiazolinone hydrazone and 2-hydroxy-1-naphthaldehyde. **BTN** can work as one of a few benzothiazole-based fluorescent “turn-on” probe for detecting Cu^{2+}, while the number of benzothiazole-based fluorescent “turn-off” sensors have been addressed. Limit of detection for Cu^{2+} was 3.3 μM. In particular, in samples with metal ions like Hg^{2+}, Fe^{3+}, Co^{2+} and Ni^{2+} having a fluorescent quenching property, **BTN** can selectively sense Cu^{2+}. Detection process of Cu^{2+} by **BTN** was demonstrated to be CHEF and ICT processes through theoretical calculations.

Declarations

Acknowledgments

The National Research Foundation of Korea (NRF) (2018R1A2B6001686 and NRF-2020R1A6A1A03042742) is gratefully acknowledged.

Availability of Data and Material (Data Transparency) Not applicable.

Code Availability (Software Application or Custom Code) Not applicable.

Authors’ Contributions Gyeongjin Kim (60% contributions), Donghwan Choi (10% contributions), Cheal Kim (30% contributions).

Declarations The authors declare that they have no known competing financial interests or personal relationships that could have appeared to influence the work reported in this paper.

References

1. Zhao Y, Zhang XB, Han ZX et al (2009) Highly sensitive and selective colorimetric and off-on fluorescent chemosensor for Cu^{2+} in aqueous solution and living cells. Anal Chem 81:7022–7030
2. Tapiero H, Townsend DM, Tew KD (2003) Trace elements in human physiology and pathology. Copper Biomed Pharmacother 57:386–398

3. Lee DY, Singh N, Jang DO (2010) A benzimidazole-based single molecular multianalyte fluorescent probe for the simultaneous analysis of Cu^{2+} and Fe^{3+}. Tetrahedron Lett 51:1103–1106
4. Que EL, Domaille DW, Chang CJ (2008) Metals in neurobiology: Probing their chemistry and biology with molecular imaging. Chem Rev 108:1517–1549
5. Smith DP, Ciccotosto GD, Tew DJ et al (2007) Concentration dependent Cu^{2+} induced aggregation and dityrosine formation of the Alzheimer's disease amyloid-βpeptide. Biochemistry 46:2881–2891
6. You GR, Lee JJ, Choi YW et al (2016) Experimental and theoretical studies for sequential detection of copper(II) and cysteine by a colorimetric chemosensor. Tetrahedron 72:875–881
7. Gaetke LM, Chow CK (2003) Copper toxicity, oxidative stress, and antioxidant nutrients. Toxicology 189:147–163
8. Seo H, An M, Kim BY et al (2017) Highly selective fluorescent probe for sequential recognition of copper(II) and iodide ions. Tetrahedron 73:4684–4691
9. Hwang SM, Chae JB, Kim C (2018) A Phenanthroimidazole-based Fluorescent Turn-Off Chemosensor for the Selective Detection of Cu^{2+} in Aqueous Media. Bull Korean Chem Soc 39:925–930
10. Na YJ, Choi YW, Yun JY et al (2015) Dual-channel detection of Cu^{2+} and F^{-} with a simple Schiff-based colorimetric and fluorescent sensor. Spectrochim Acta - Part A Mol Biomol Spectrosc 136:1649–1657
11. Lee HJ, Park SJ, Sin HJ et al (2015) A selective colorimetric chemosensor with an electron-withdrawing group for multi-analytes $CN^{-}$and F^{-}. New J Chem 39:3900–3907
12. Goswami S, Sen D, Das NK (2010) A new highly selective, ratiometric and colorimetric fluorescence sensor for Cu^{2+} with a remarkable red shift in absorption and emission spectra based on internal charge transfer. Org Lett 12:856–859
13. Shivaprasad M, Govindaraju T (2011) Rhodamine based bright red colourimetric and turn-on fluorescence chemosensor for selective detection of Cu^{2+}. Mater Technol 26:168–172
14. Jiao Y, Zhou L, He H et al (2018) A novel rhodamine B-based "off-on" fluorescent sensor for selective recognition of copper (II) ions. Talanta 184:143–148
15. Rout K, Manna AK, Sahu M et al (2019) Triazole-based novel bis Schiff base colorimetric and fluorescent turn-on dual chemosensor for Cu^{2+} and Pb^{2+}: Application to living cell imaging and molecular logic gates. RSC Adv 9:25919–25931
16. Li Y, Lan H, Yan X et al (2020) Retinal-based polyene fluorescent probe for selectively detection of Cu^{2+} in physiological saline and serum. Spectrochim Acta - Part A Mol Biomol Spectrosc 227:117565
17. Ko KC, Wu JS, Kim HJ et al (2011) Rationally designed fluorescence 'turn-on' sensor for Cu^{2+}. Chem Commun 47:3165–3167
18. Feng S, Gao Q, Gao X et al (2019) Fluorescent sensor for copper(II) ions based on coumarin derivative and its application in cell imaging. Inorg Chem Commun 102:51–56

19. Lv XL, Wei Y, Luo SZ (2012) A “turn-on” fluorescent chemosensor based on peptidase for detecting copper. Anal Sci 28:749–752
20. Wang J, Zong Q (2015) A new turn-on fluorescent probe for the detection of copper ion in neat aqueous solution. Sensors Actuators B Chem 216:572–577
21. Mal K, Naskar B, Chaudhuri T et al (2020) Synthesis of quinoline functionalized fluorescent chemosensor for Cu (II), DFT studies and its application in imaging in living HEK 293 cells. J Photochem Photobiol A Chem 389:112211
22. Chen Z, Wang L, Zou G et al (2013) Highly selective fluorescence turn-on chemosensor based on naphthalimide derivatives for detection of copper(II) ions. Spectrochim Acta - Part A Mol Biomol Spectrosc 105:57–61
23. Bhaskar R, Kumar GGV, Sivaraman G et al (2019) Fluorescence “turn-on” sensor for highly selective recognition of Cu^{2+} ion and its application to living cell imaging. Inorg Chem Commun 104:110–118
24. Xiao-Ni Q, Dang LR, Qu WJ et al (2020) Phenazine derivatives for optical sensing: A review. Royal Society of Chemistry
25. Helal A, Or Rashid MH, Choi CH, Kim HS (2011) Chromogenic and fluorogenic sensing of Cu^{2+} based on coumarin. Tetrahedron 67:2794–2802
26. Li Z, Chen QY, Wang PD, Wu Y (2013) Multifunctional BODIPY derivatives to image cancer cells and sense copper(ii) ions in living cells. RSC Adv 3:5524–5528
27. Kumar A, Datta LP, Samanta S et al (2021) Benzothiazole-phenothiazine Conjugate Based Molecular Probe for the Differential Detection of Glycated Albumin. Isr J Chem 1–10
28. Sik Na W, Raj P, Singh N, Jang DO (2019) Benzothiazole-based heterodipodal chemosensor for Cu^{2+} and CN^{-} ions in aqueous media. Tetrahedron Lett 60:151075
29. Lee SA, Lee JJ, Shin JW et al (2015) A colorimetric chemosensor for the sequential detection of copper(II) and cysteine. Dye Pigment 116:131–138
30. Wu JS, Wang PF, Zhang XH, Wu SK (2006) Novel fluorescent sensor for detection of Cu(II) in aqueous solution. Spectrochim Acta - Part A Mol Biomol Spectrosc 65:749–752
31. Xiao N, Xie L, Zhi X, Fang CJ (2018) A naphthol-based highly selective fluorescence turn-on and reversible sensor for Al(III) ion. Inorg Chem Commun 89:13–17
32. Shen Y, Zhang X, Zhang C et al (2018) A simple fluorescent probe for the fast sequential detection of copper and biothiols based on a benzothiazole derivative. Spectrochim Acta - Part A Mol Biomol Spectrosc 191:427–434
33. Kim D, Bin, Lee KH, Park KY et al (2018) Masking agent-controlled discriminative Hg^{2+} and Cu^{2+} sensing by quinonediimine dye formation of aniline-functionalized silica nanoparticles. Sensors Actuators B Chem 259:847–854
34. Wang H, Zhao S, Xu Y et al (2020) A new fluorescent probe based on imidazole[2,1-b]benzothiazole for sensitive and selective detection of Cu^{2+}. J Mol Struct 1203:127384

35. Nandre J, Patil S, Patil V et al (2014) A novel fluorescent “turn-on” chemosensor for nanomolar detection of Fe(III) from aqueous solution and its application in living cells imaging. Biosens Bioelectron 61:612–617
36. Chang C, Wang F, Wei T, Chen X (2017) Benzothiazole-Based Fluorescent Sensor for Ratiometric Detection of Zn(II) Ions and Secondary Sensing PPi and Its Applications for Biological Imaging and PPase Catalysis Assays. Ind Eng Chem Res 56:8797–8805
37. Jayabharathi J, Ramanathan P, Thanikachalam V, Arunpandiyan A (2014) Sensitive and selective PET-based π-expanded phenanthrimidazole luminophore for Zn^{2+} ion. J Fluoresc 24:827–834
38. Li Z, Liu C, Wang J et al (2019) A selective diaminomaleonitrile-based dual channel emissive probe for Al^{3+} and its application in living cell imaging. Spectrochim Acta - Part A Mol Biomol Spectrosc 212:349–355
39. Dolai B, Bhaumik A, Pramanik N et al (2018) Naphthaldimine-based simple glucose derivative as a highly selective sensor for colorimetric detection of Cu^{2+} ion in aqueous media. J Mol Struct 1164:370–377
40. Lim MH, Wong BA, Pitcock WH et al (2006) Direct nitric oxide detection in aqueous solution by copper(II) fluorescein complexes. J Am Chem Soc 128:14364–14373
41. Dong HQ, Wei TB, Ma XQ et al (2020) 1,8-Naphthalimide-based fluorescent chemosensors: recent advances and perspectives. J Mater Chem C 8:13501–13529
42. Magde D, Wong R, Seybold PG (2002) Fluorescence Quantum Yields and Their Relation to Lifetimes of Rhodamine 6G and Fluorescein in Nine Solvents: Improved Absolute Standards for Quantum Yields. Photochem Photobiol 75:327
43. Frisch MJ, Trucks GW, Schlegel HB, Scuseria GE, Robb MA, Cheeseman JR, Scalmani G, Barone V, Mennucci B, Petersson GA, Nakatsuji H, Caricato M, Li X, Hratchian HP, Izmaylov AF, Bloino J, Zheng G, Sonnenberg JL, M. Had 2009). G09 | Gaussian.com
44. Becke AD (1993) Density-functional thermochemistry. III. The role of exact exchange. J Chem Phys 98:5648–5652
45. Lee C, Yang W, Parr RG (1988) Development of the Colle-Salvetti correlation-energy formula into a functional of the electron density. Phys Rev B 37:785–789
46. Hariharan PC, Pople JA (1973) The influence of polarization functions on molecular orbital hydrogenation energies. Theor Chim Acta 28:213–222
47. Francl MM, Pietro WJ, Hehre WJ et al (1982) Self-consistent molecular orbital methods. XXIII. A polarization-type basis set for second-row elements. J Chem Phys 77:3654–3665
48. Hay PJ, Wadt WR (1985) Ab initio effective core potentials for molecular calculations. Potentials for the transition metal atoms Sc to Hg. J Chem Phys 82:270–283
49. Wadt WR, Hay PJ (1985) Ab initio effective core potentials for molecular calculations. Potentials for main group elements Na to Bi. J Chem Phys 82:284–298

50. Hay PJ, Wadt WR (1985) *Ab initio* effective core potentials for molecular calculations. Potentials for K to Au including the outermost core orbitals. J Chem Phys 82:299–310
51. Klamt A, Moya C, Palomar J (2015) A Comprehensive Comparison of the IEFPCM and SS(V)PE Continuum Solvation Methods with the COSMO Approach. J Chem Theory Comput 11:4220–4225
52. Mukhopadhyay M, Banerjee D, Koll A et al (2005) Excited state intermolecular proton transfer and caging of salicylidine-3,4,7-methyl amine in cyclodextrins. J Photochem Photobiol A Chem 175:94–99
53. Goswami S, Aich K, Das S et al (2015) A new visible-light-excitable ICT-CHEF-mediated fluorescence “turn-on” probe for the selective detection of Cd^{2+} in a mixed aqueous system with live-cell imaging. Dalton Trans 44:5763–5770
54. Slassi S, Aarjane M, El-Ghayoury A, Amine A (2019) A highly turn-on fluorescent CHEF-type chemosensor for selective detection of Cu^{2+} in aqueous media. Spectrochim Acta - Part A Mol Biomol Spectrosc 215:348–353
55. Chang Y, Li B, Mei H et al (2020) Indole-based colori/fluorimetric probe for selective detection of Cu^{2+} and application in living cell imaging. Spectrochim Acta - Part A Mol Biomol Spectrosc 226:117631

Supplementary Information

Supplementary Information files were not provided with this version of the manuscript.

Figures

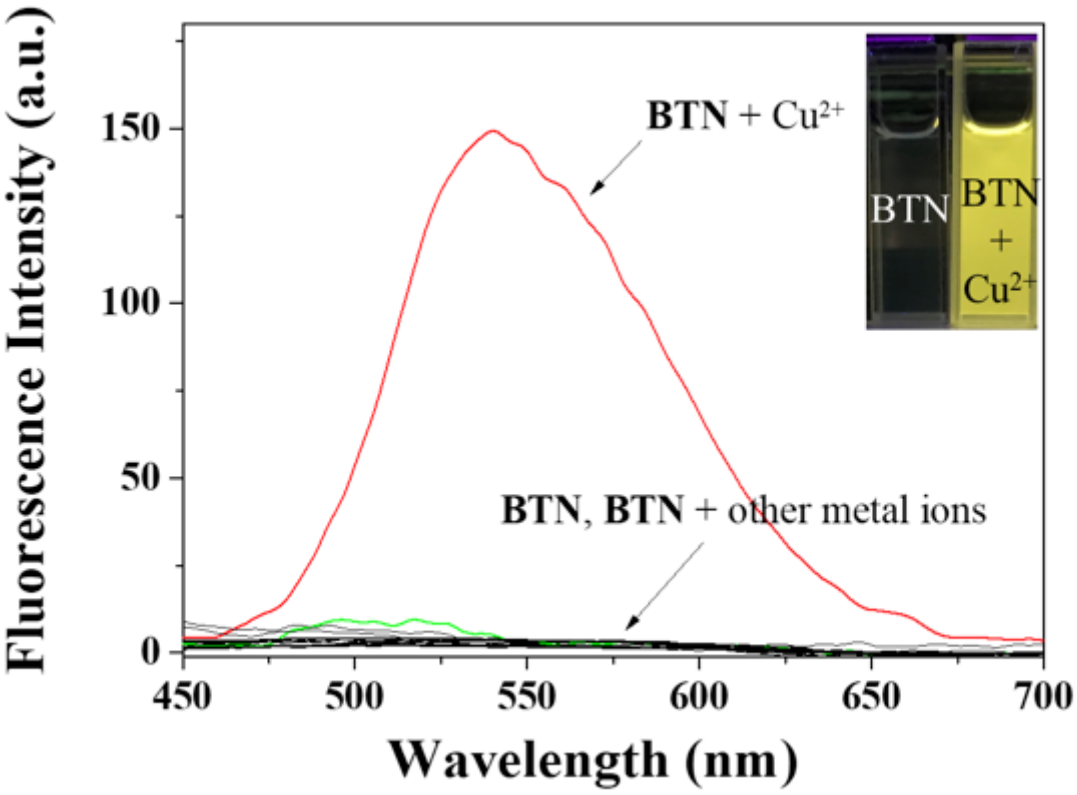

Figure 1

Fluorescent response of BTN to diverse cations. Inset: Fluorescent image of BTN and BTN-Cu2+.

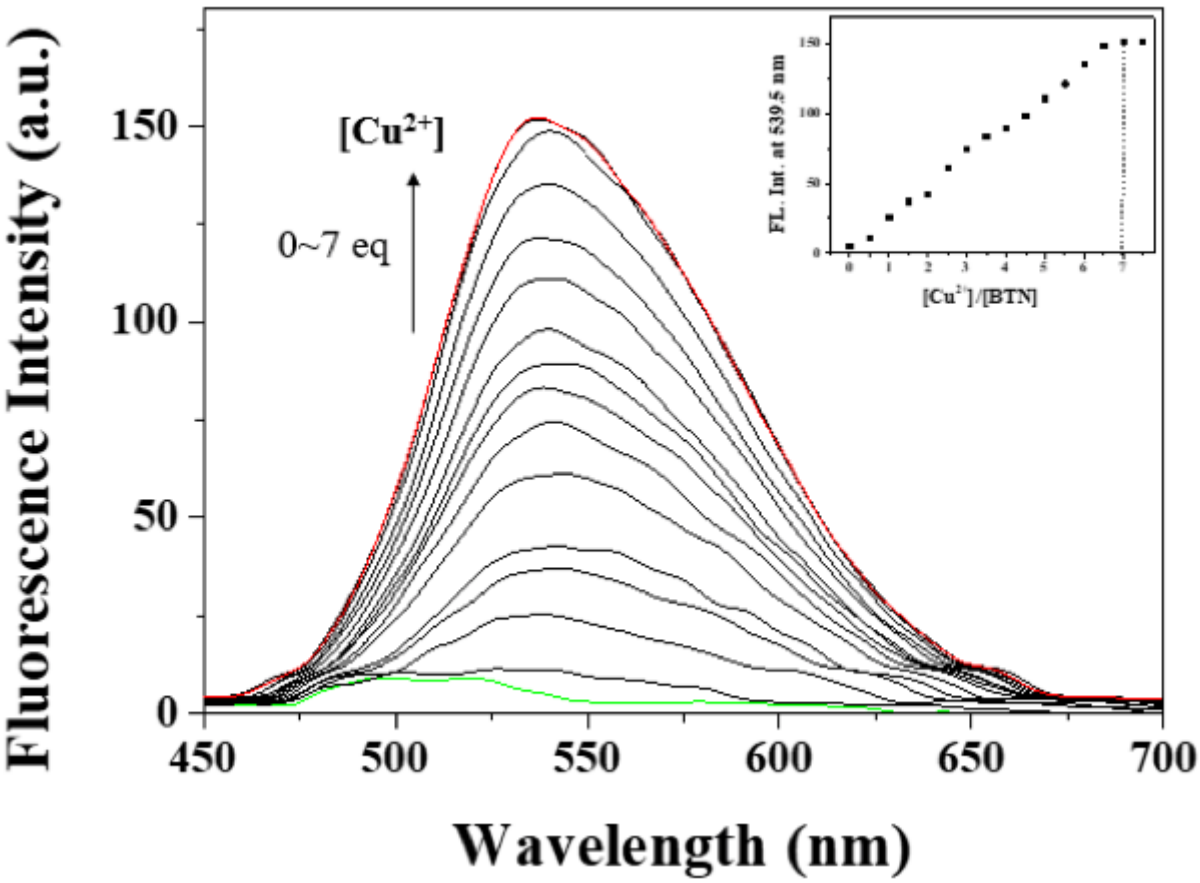

Figure 2

Fluorescent variations of BTN (1x10-5 M) with different concentrations of Cu2+.

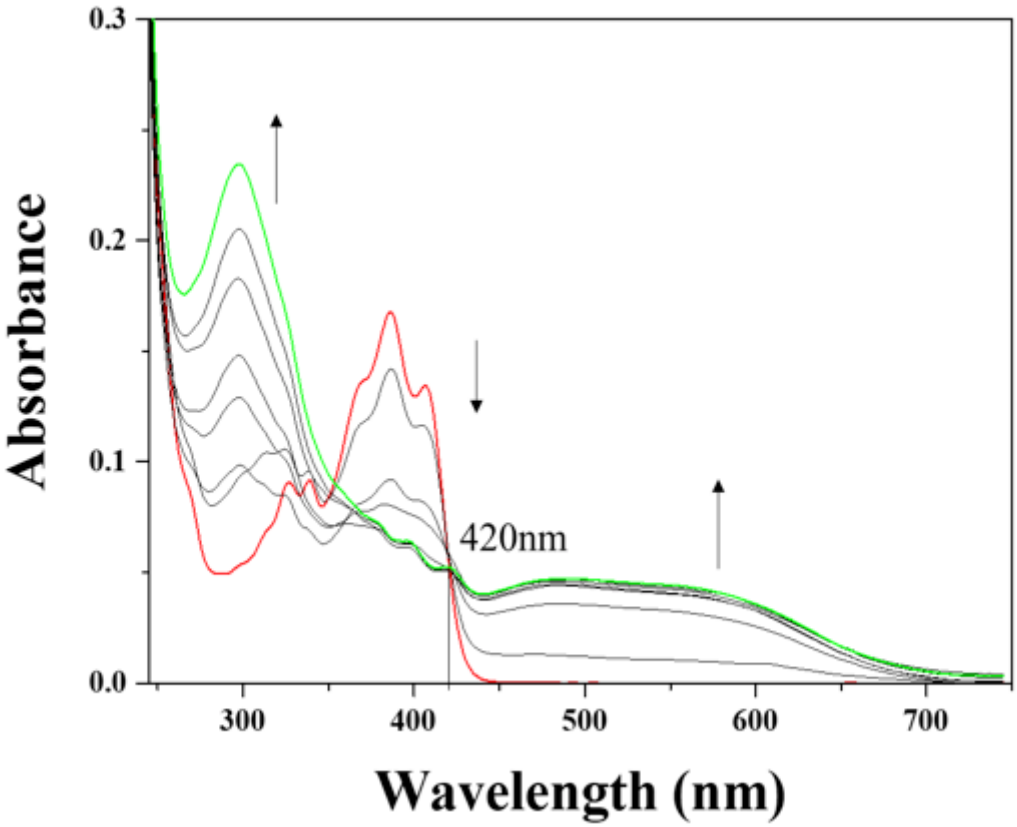

Figure 3

Absorption spectral changes of BTN (10μM) with increment of Cu2+.

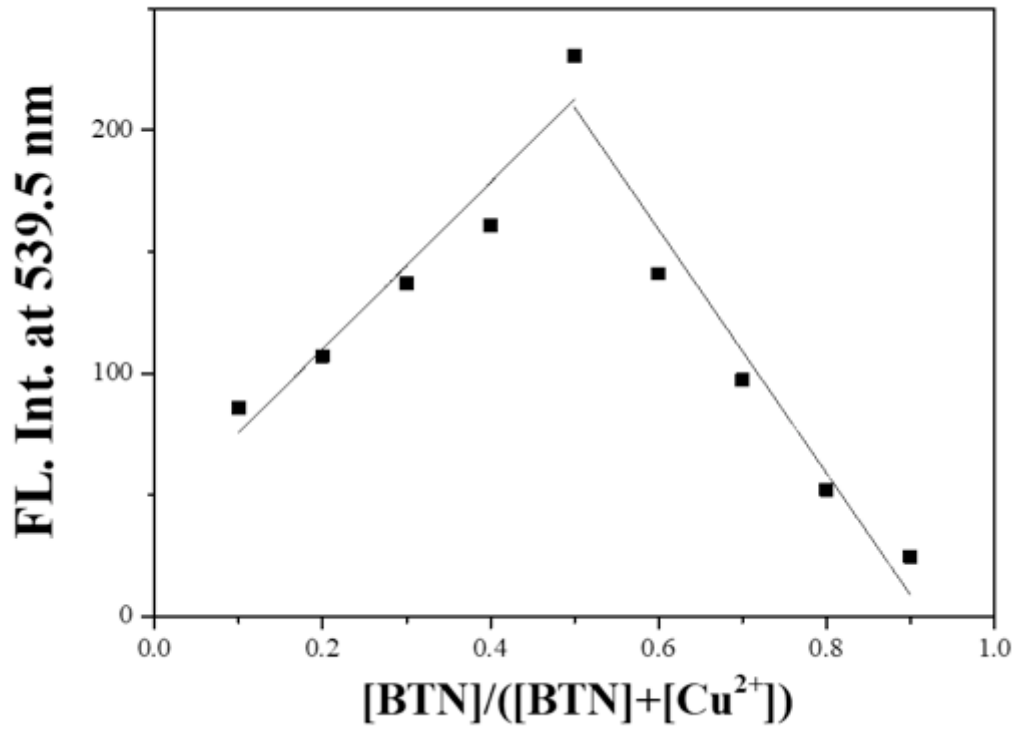

Figure 4

Job plot analysis of BTN with Cu2+.

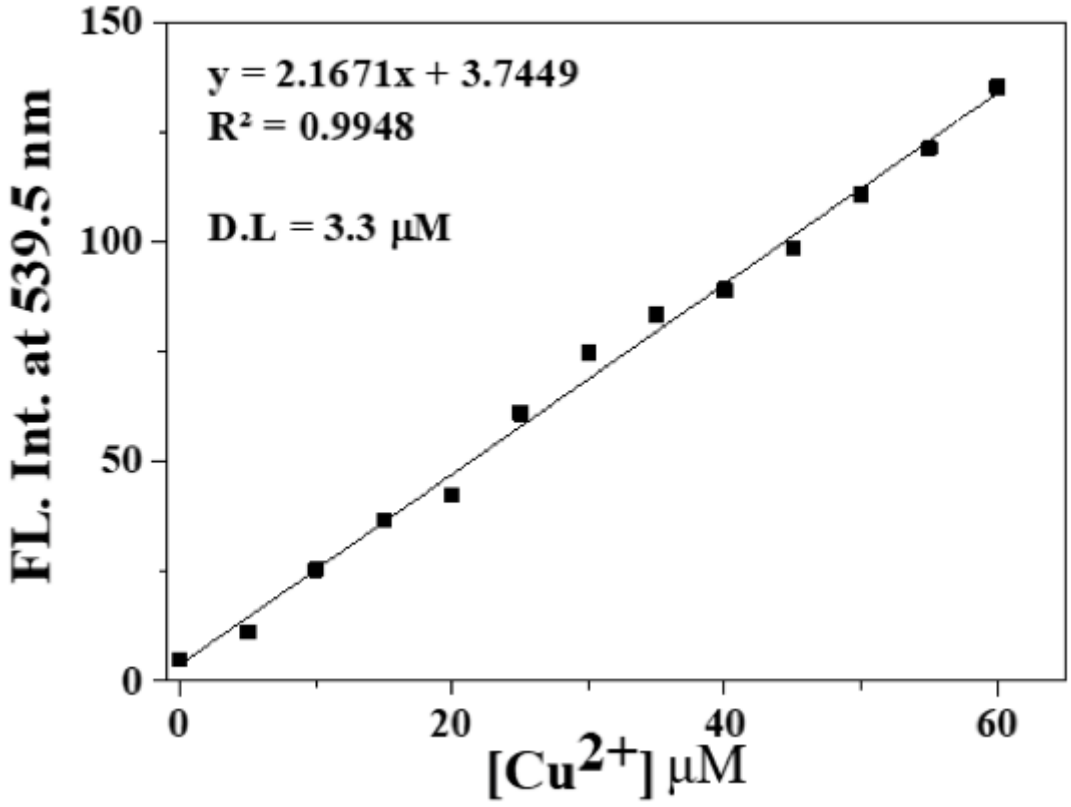

Figure 5

Detection limit of BTN (1x10-5 M) for Cu2+.

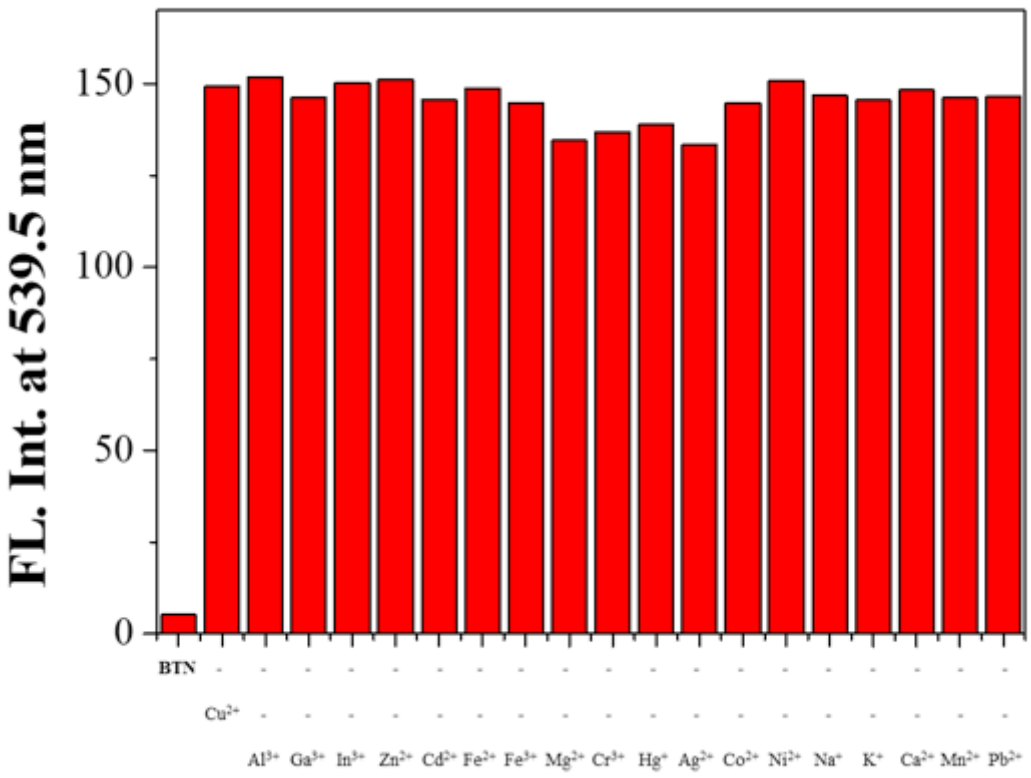

Figure 6

Fluorescence intensity of BTN and Cu2+ with other cations.

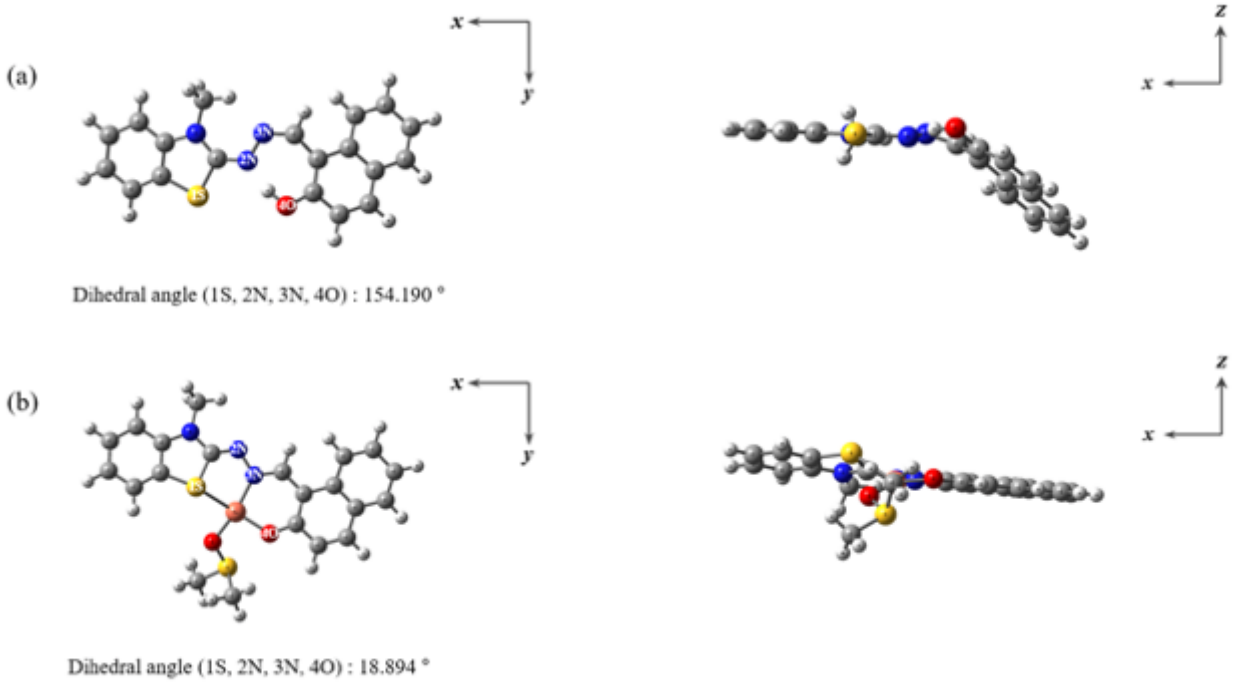

Figure 7

Energy-optimized forms of (a) BTN and (b) BTN-Cu2+.

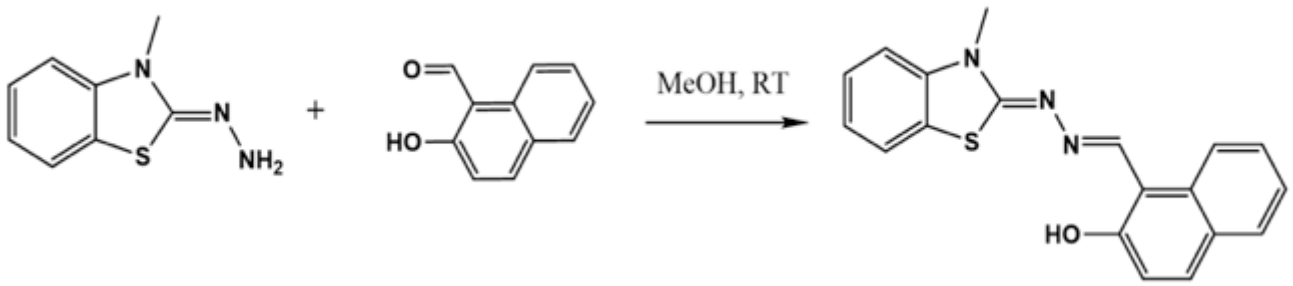

Figure 8

Scheme 1. Synthesis of BTN.

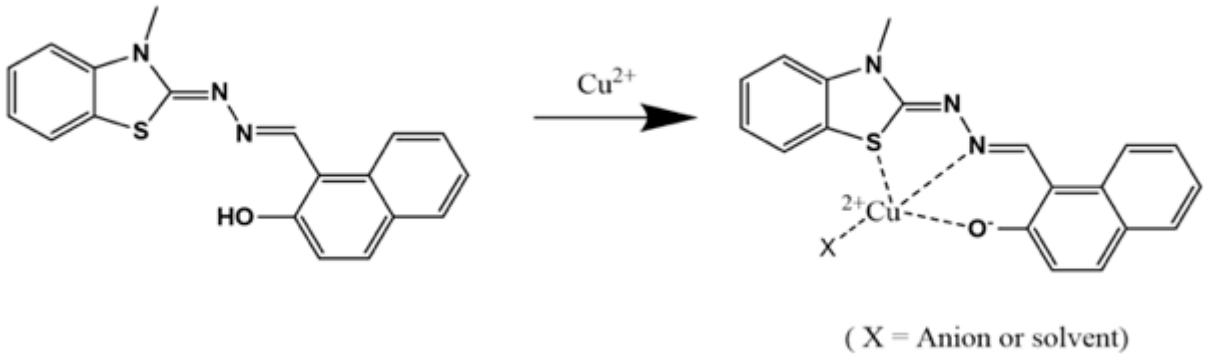

Figure 9

Scheme 2. Response process of BTN to Cu2+.